2022 IEEE International Conference on Environment and Electrical Engineering and 2022 IEEE Industrial and Commercial Power Systems Europe (EEEIC / I&CPS Europe) | 978-1-6654-8537-1/22/$31.00 ©2022 IEEE | DOI: 10.1109/EEEIC/ICPSEUROPE54979.2022.9854611

Volt-Var Optimization with Power Management of Plug-in Electric Vehicles for Conservation Voltage Reduction in Distribution Systems

Darwin A. Quijano
São Paulo State University-UNESP
Ilha Solteira, SP, Brazil
alexisqr@yahoo.es

Antonio Padilha-Feltrin
São Paulo State University-UNESP
Ilha Solteira, SP, Brazil
antonio.padilha-feltrin@unesp.br

João P. S. Catalão
University of Porto and INESC TEC
Porto, Portugal
catalao@fe.up.pt

***Abstract*—This paper addresses the problem of Volt-Var optimization for conservation voltage reduction (CVR) implementation in medium voltage electric distribution systems (EDS) with high penetration levels of renewable energy sources (RES)-based distributed generation (DG). The proposed strategy seeks to coordinate the power dispatch of aggregated electric vehicles (EVs) for EDS voltage control taking into account technical characteristics and the driving patterns of individual EVs. The strategy is for the day-ahead operation scheduling, where decisions are made based on predictions of RES-based DG power production, conventional load consumption and EV driving patterns. Forecast errors are taken into account through a two-stage stochastic programming formulation, where probability density functions are used to describe the uncertainties of predicted parameters. Simulations were carried out on a 33-bus test system and results showed energy savings of up to 3% when EVs participate in voltage control.**

***Index Terms*—Conservation voltage reduction, electric vehicles, renewable energy sources.**

I. Introduction

Conservation voltage reduction (CVR) is the procedure of reducing the voltage levels in electric distribution systems (EDSs) to induce a reduction in the consumption of voltage dependent loads [1]. CVR is a demand response resource that the distribution system operators (DSOs) can access as long as there is the possibility of reducing the EDS voltage levels within the statutory limits. However, voltage control in EDSs with high levels of renewable energy sources (RES)-based distributed generation (DG) is a complex task due to the variability and uncertainty of power production.

Voltage control in EDSs is usually performed using traditional voltage regulation and reactive power support devices such as on-load tap changers (OLTCs), distributed voltage regulators, and capacitor banks. For example, a common approach for implementing CVR uses an OLTC line drop compensation method to reduce the secondary voltage of the substation [2]. Fields tests of CVR implementation have reported 0.3% to 1% load reduction per 1% voltage reduction [3]. The modernization of EDSs through the upgrading of computation and communication technologies has opened the possibility of integrating CVR into Volt-Var optimization (VVO) models as an objective function, thus increasing the CVR gains [1], [4]. VVO models are developed to optimally coordinate the operation of Volt-Var control devices to achieve one or more EDS operating objectives [5].

The voltage regulation capability of traditional Volt-Valt control devices is limited by their slow time response, discrete features, and limited number of switching operations. These disadvantages restrict the gains that can achieved through CVR in EDSs with high penetration levels of RES-based DG due to fast and uncertain voltage fluctuations. Therefore, to improve the performance of CVR implementation, modern VVO models have been designed to include optimal control of PV smart inverters [6], [7], battery energy storage systems [8], [9], and demand response [10].

Given the increasing penetration of plug-in electric vehicles (EVs) in EDSs, optimal EVs charging coordination has been proposed as a solution for the optimized EDSs operation [11]. Further, EVs can operate as vehicle-to-grid (V2G) devices injecting power into the EDS, which allows the provision of ancillary services like load shifting, peak shaving, spinning reserve, and voltage regulation [12]. However, only two works were found where the implementation of CVR in EDSs with EVs is investigated [13], [14]. In [13] it is proposed a VVO model that takes into account the impact of different EV charging loads with the ability of participating in reactive power support, but without considering optimal charging. In [14], EV charging is optimized to reduce the energy consumption through CVR, however, without considering the presence of RES-based DG and V2G operation. In addition, [13], [14] do not take into account uncertainties related to EV driving patterns.

This work seeks to address the problem of CVR implementation in medium voltage (MV) EDSs taking advantage of the controllable characteristics of EVs. An aggregated model of EVs that takes into account technical specifications and driving patterns of individual EVs is proposed. The problem is formulated from the point of view of the DSO who centrally decides the power dispatch of the EVs aggregated at specific EDS buses. The strategy is for

This work was supported by São Paulo Research Foundation (FAPESP) under grants: 2018/06451-8, 2020/12401-3 and 2015/21972-6, by National Council for Scientific and Technological Development under grant: 310299/2020-9.

the day-ahead operation scheduling, where decisions are made based on predictions of RES-based DG power production, conventional load consumption, and EV driving patterns. Moreover, prediction errors are taken into account through a two-stage stochastic programming formulation.

The contributions of this work as summarized as follows:

- A novel strategy that takes advantage of the controllability of EVs (including V2G operation) for CVR implementation in MV EDSs with high penetration of RES-based DG. To the best of the authors' knowledge, this is the first time that it is proposed to coordinate the dispatch of EVs to regulate bus voltages for CVR implementation in EDSs with high penetration of RES-based DG.
- A VVO model formulated as a two-stage stochastic programming problem to coordinate the dispatch of aggregated EVs and the OLTC operation for CVR implementation. This formulation is proposed to simultaneously take into account uncertainties of RES-based DG power production (including solar PV and wind), conventional load consumption, and EVs driving patterns in the CVR problem, which has not been done before.

II. Mathematical model

This section presents the mathematical formulation that models the problem of controlling the voltage levels for energy conservation in distribution systems. The problem is formulated for the day-ahead operation scheduling of EDSs, and uncertainties are taken into account adopting a two-stage stochastic programming formulation. First-stage decisions correspond to the OLTC tap settings, which must hold for all possible uncertainty realizations because of their slow response and discrete nature. The power absorbed and injected by the EVs aggregated at specific buses correspond to the second-stage decisions, which are adjusted according to the uncertainty realizations. Prediction errors of renewable-based DG power production, conventional demand, and EV driving patterns are characterized using PDFs from which a set of representative scenarios (uncertainty realizations) is sampled. In the following formulation the indices $s \in \Omega_s$, $t \in \Omega_t$, $i \in \Omega_b$, and $ij \in \Omega_l$ correspond to scenarios, hours, buses, and line segments, respectively. Ω_s, Ω_t, Ω_b, and Ω_l denote the sets of scenarios, hours, buses and line segments.

A. Objective function

The objective function is formulated to minimize expected value of the energy consumption of voltage dependent loads plus energy losses in distribution lines during the day as follows:

$$min: \sum_{s\in\Omega_s} \rho_s \sum_{t\in\Omega_t} \tau \left(\sum_{i\in\Omega_b} P^l_{i,t,s} + \sum_{ij\in\Omega_l} r_{ij} I^{sqr}_{ij,t,s} \right). \quad (1)$$

where, ρ_s, $P^l_{i,t,s}$, r_{ij}, and $I^{sqr}_{ij,t,s}$ denote the scenario probability, conventional load active power, resistance of line segments, and magnitude of the current squared in line segments. τ indicates the duration of the time interval, which in this work is equal to one hour.

B. Voltage dependent loads

The voltage dependent behavior of loads is modeled using the ZIP model as follows:

$$P^l_{i,t,s} = P^Z_{i,t,s} V^2_{i,t,s} + P^I_{i,t,s} V_{i,t,s} + P^P_{i,t,s}, \quad (2)$$

$$Q^l_{i,t,s} = Q^Z_{i,t,s} V^2_{i,t,s} + Q^I_{i,t,s} V_{i,t,s} + Q^P_{i,t,s}. \quad (3)$$

This model describes loads as a combination of constant impedance (Z), constant current (I), and constant power (P) components. The participation of each component in the total load active (reactive) power is given by $P^Z_{i,t,s}$, $P^I_{i,t,s}$, and $P^P_{i,t,s}$ ($Q^Z_{i,t,s}$, $Q^I_{i,t,s}$, and $Q^P_{i,t,s}$). These components are uncertain parameters modeled through PDFs as will be shown later. $Q^l_{i,t,s}$ and $V_{i,t,s}$ denote the conventional load reactive power and the magnitude of the bus voltage, respectively.

C. Distributed generation

This work considers the presence of solar PV and wind-based DG in the EDS. The active power supplied by these generation technologies is given by

$$P^w_{i,t,s} = \omega^w_{t,s} S^w_i, \quad (4)$$

$$P^{pv}_{i,t,s} = \omega^{pv}_{t,s} S^{pv}_i, \quad (5)$$

where, $P^w_{i,t,s}$ and $P^{pv}_{i,t,s}$ indicate the active power supplied by the wind-based DG and the solar PV-based DG, respectively. $\omega^w_{t,s}$ and $\omega^{pv}_{t,s}$ denote the normalized active power of the wind-based DG and the solar PV-based DG, respectively. These are uncertain parameters described by PDFs as will be shown in the next section. S^w_i and S^{pv}_i are the rated capacity of the wind-based DG and solar PV-based DG, respectively.

D. Aggregated EV model

The proposed approach takes advantage of the controllability of EVs to regulate bus voltages and induce a reduction in the energy consumption of voltage dependent loads and energy losses. EVs are assumed as clustered at particular buses and their aggregated impact on the distribution system is investigated. The determination of the charging schedule of individual EVs is relegated to distributed controllers and will no be considered in this work.

In this work, the problem is formulated from the point of view of the DSO who determines the power to be absorbed from or injected into de EDS by the aggregated EVs at each node and time interval. The charging schedules of individual EVs are considered to be estimated in a distributed way taking into account the energy needs of the EVs and the DSO. The DSO schedules the power to be injected and absorbed by the aggregated EVs at each node and time interval aware of the number of EVs plugged in and their SOC. This information is forecasted by the DSO to model each aggregated collection of EVs as a virtual storage device whose power and energy capacities are uncertain and dynamic [11]. Thus, the DSO dispatch the aggregated EVs taking into account their capacity

bounds and the energy requirements of individual EVs. The dispatch of aggregated EVs is modeled as follows:

$$E_{i,t,s} = E_{i,t-1,s} + E^{arr}_{i,t,s} - E^{dep}_{i,t,s} + \eta^{+}\tau P^{ev^{+}}_{i,t,s} \frac{1}{\eta^{-}} \tau P^{ev^{-}}_{i,t,s}, \quad (6)$$

$$0 \le E_{i,t,s} \le E^{\max}_{i,t,s}, \quad (7)$$

$$0 \le P^{ev^{+}}_{i,t,s} \le z^{+}_{i,t,s} \overline{P}^{ev^{+}}_{i,t,s}, \quad (8)$$

$$0 \le P^{ev^{-}}_{i,t,s} \le z^{-}_{i,t,s} \overline{P}^{ev^{-}}_{i,t,s}, \quad (9)$$

$$z^{-}_{i,t,s} + z^{+}_{i,t,s} \le 1, \quad (10)$$

where, (6) models the dynamic energy balance of the aggregated EVs. The energy stored by the EVs aggregated at bus i ($E_{i,t,s}$) at each time interval t depends on the energy stored at the previous time interval $t-1$ ($E_{i,t-1,s}$), the energy increase due to EVs arriving ($E^{arr}_{i,t,s}$), the energy drop due to EVs departing ($E^{dep}_{i,t,s}$), the energy absorbed from the EDS ($\eta^{+}\tau P^{ev^{+}}_{i,t,s}$) and the energy injected into the EDS ($\tau P^{ev^{-}}_{i,t,s}/\eta^{-}$). η^{+} and η^{-} indicate the charging and discharging efficiencies of individual EVs. The stored energy ($E_{i,t,s}$), power absorbed by the aggregated EVs ($P^{ev^{+}}_{i,t,s}$), and power injected by the aggregated EVs ($P^{ev^{-}}_{i,t,s}$) are constrained in (7)-(9) to minimum and maximum values. $E^{\max}_{i,t,s}$, $\overline{P}^{ev^{+}}_{i,t,s}$, and $\overline{P}^{ev^{-}}_{i,t,s}$ indicate the maximum storage capacity, maximum power absorption, and maximum power injection of the aggregated EVs. The binary variables $z^{-}_{i,t,s}$ and $z^{+}_{i,t,s}$ define the operation status of the aggregated EVs. Constraint (10) prevents the EVs to absorb and inject power simultaneously.

The power and energy limits of the EVs aggregated at bus i, for each time interval t and scenario s, are calculated taking into account the connection status and SOC of every EV as follows:

$$E^{\max}_{i,t,s} = \sum_{m \in M_i} E^{cap}_{m} f_{m,t,s}, \quad (11)$$

$$\overline{P}^{ev^{+}}_{i,t,s} = \sum_{m \in M_i} \hat{P}^{ev^{+}}_{m} f_{m,t,s}, \quad (12)$$

$$\overline{P}^{ev^{-}}_{i,t,s} = \sum_{m \in M_i} \hat{P}^{ev^{-}}_{m} f_{m,t,s}, \quad (13)$$

$$E^{arr}_{i,t,s} = \sum_{m \in M_i} E^{ini}_{m,s} g^{arr}_{m,t,s}, \quad (14)$$

$$E^{dep}_{i,t,s} = \sum_{m \in M_i} E^{cap}_{m} g^{dep}_{m,t,s}, \quad (15)$$

where, (11) calculates the maximum storage capacity of the aggregated EVs as the sum of the battery capacities of individual EVs (E^{cap}_{m}). (12) and (13) calculate the upper limits of power absorbed and injected by the aggregated EVs as the sum of the maximum charging ($\hat{P}^{ev^{+}}_{m}$) and discharging ($\hat{P}^{ev^{-}}_{m}$) powers of individual EVs. $f_{m,t,s}$ is a binary parameter that indicates if an EV m is plugged into the EDS at time interval t and scenario s. The value taken by $f_{m,t,s}$ is determined by the times when the EV m arrives ($t^{arr}_{m,s}$) and departs ($t^{dep}_{m,s}$). $t^{arr}_{m,s}$ and $t^{dep}_{m,s}$ are uncertain parameters modeled using PDFs as will by shown in the following section. M_i indicates the set of EVs aggregated at bus i.

Constraints (14) and (15) determine the increase and decrease in the energy stored by the aggregated EVs due to EVs arriving and departing at time t, respectively. The binary parameter $g^{arr}_{m,t,s}$ in (14) takes the value 1 at time interval $t^{arr}_{m,s}$ when the EV m arrives and is plugged in, and takes the value 0 at other time intervals. In (15), the binary parameter $g^{dep}_{m,t,s}$ takes the value 1 at time interval $t^{dep}_{m,s}$ when the EV m is plugged out and departs, and takes the value 0 at other time intervals. The SOC $E^{ini}_{m,s}$ of the EV m at the arriving time is determined by the consumption per mile and the daily travel mileage ($\chi_{m,s}$), which is an uncertain parameter modeled using a PDF. Constraint (15) establishes that EVs depart with the battery at full capacity E^{cap}_{m}.

E. OLTC model

The model adopted for the OLTC is defined as follows:

$$V_{i,t,s} = \tilde{V}_{i,t,s} + \Delta tap_i tap_{i,t}, \quad (16)$$

$$-\overline{tap}_i \le tap_{i,t} \le \overline{tap}_i, \quad (17)$$

$$\lambda^{R}_{i,t} \ge tap_{i,t+1} - tap_{i,t}, \quad (18)$$

$$\lambda^{R}_{i,t} \ge tap_{i,t} - tap_{i,t+1}, \quad (19)$$

$$\sum_{t \in \Omega_t} \lambda^{R}_{i,t} \le N^{tp}_{i}. \quad (20)$$

In the above formulation, (16) indicates that the voltage $V_{i,t,s}$ at the regulated end of the OLTC is equal to the voltage $\tilde{V}_{i,t,s}$ at the non-regulated end plus the adjustment $\Delta tap_i tap_{i,t}$. Δtap_i denotes the step of voltage variation per switching operation, and $tap_{i,t}$ the tap position, which is a control variable that must hold for all scenarios s. Constraint (17) defines the range of variation of the tap position, limited by minimum ($\overline{tap}_i$) and maximum ($\overline{tap}_i$) values. The number of switching operation of the OLTC during the day are limited to a maximum value N^{tp}_{i} in (18)-(20). In this formulation, $\lambda^{R}_{i,t}$ is an auxiliary variable that indicates the number of switching operations between the two consecutive time intervals.

F. Power balance equations

The power power flows at each node i are described using the DistFlow equations [15] as follows:

$$\sum_{ij \in \Omega_l} P_{ij,t,s} = P_{hi,t,s} - r_{hi} I^{sqr}_{hi,t,s} - P^{l}_{i,t,s} - P^{ev^{+}}_{i,t,s} + P^{ex}_{i,t,s} + P^{ev^{-}}_{i,t,s} + P^{w}_{i,t,s} + P^{pv}_{i,t,s}, \quad (21)$$

$$\sum_{ij \in \Omega_l} Q_{ij,t,s} = Q_{hi,t,s} - x_{hi} I^{sqr}_{hi,t,s} - Q^{l}_{i,t,s} + Q^{ex}_{i,t,s}, \quad (22)$$

$$\tilde{V}_{j,t,s} = V_{i,t,s} - \left(r_{ij} P_{ij,t,s} + x_{ij} Q_{ij,t,s}\right)/V^{n2}. \quad (23)$$

$$I^{sqr}_{hi,t,s} = \left(P^{2}_{hi,t,s} + Q^{2}_{hi,t,s}\right)/V^{n2}. \quad (24)$$

$$\underline{V} \le V_{j,t,s} \le \overline{V}, \quad (25)$$

where, h is the node upstream node i and $j|ij \in \Omega_l$ is the set of nodes downstream node i for a distribution system with radial topology. $P_{ij,t,s}$ and $Q_{ij,t,s}$ indicate, respectively, the active and reactive power flow between buses i and j. $P^{ex}_{i,t,s}$ and $Q^{ex}_{i,t,s}$ denote, respectively, the active and reactive power exchange through the substation. x_{hi} indicates the reactance of

the line segment hi. $\underline{V}$ and $\overline{V}$ are, respectively, the minimum and maximum bus voltages. V^n is the nominal voltage.

G. Model convexification

The optimization model given by (1)-(25) is mixed integer nonlinear. Nonlinearities result from constraints (2), (3) and (24), which also make the problem nonconvex. Constraints (2) and (3) are covexified by applying a linear approximation based on Taylor's expansion around $V_{i,t,s} = V^n = 1.0\ p.u.$ disregarding the second and higher order terms as follows:

$$P^l_{i,t,s} = P^Z_{i,t,s}(2V_{i,t,s} - 1) + P^I_{i,t,s}V_{i,t,s} + P^P_{i,t,s} \quad (26)$$

$$Q^l_{i,t,s} = Q^Z_{i,t,s}(2V_{i,t,s} - 1) + Q^I_{i,t,s}V_{i,t,s} + Q^P_{i,t,s} \quad (27)$$

Since the problem is formulated to maintain bus voltages within a tight range around V^n, the error introduced by the approximation (26) and (27) is not too significant. Constraint (24) is convexified by relaxing the equality as follows:

$$I^{sqr}_{hi,t,s} \geq \left(P^2_{hi,t,s} + Q^2_{hi,t,s}\right)/{V^n}^2. \quad (28)$$

Sufficient conditions for this relaxation to be exact is that the bus voltage is kept close to V^n and that the power injection at each bus is not too large [16].

III. Uncertainty characterization

The proposed optimization algorithm schedules the operation of the OLTC and the dispatch of the aggregated EVs based on predictions of generation, conventional demand, and EVs travel patterns. Such predictions are subject to prediction errors, which in this work are modeled through a scenario based approach. This approach assumes that the uncertain parameters can be described by PDFs from which scenarios are sampled.

A. RES-based DG power uncertainty

The forecast errors of solar PV and wind-based DG power production are considered to be described by Beta PDFs [17]. The Beta PDF for wind-based DG is defined as follows:

$$f_{\bar{\omega}^w_t}(\omega^w_t) = \frac{{\omega^w_t}^{\alpha_t - 1} \cdot (1 - \omega^w_t)^{\beta_t - 1}}{B(\alpha_t, \beta_t)}, \quad (29)$$

$$B(\alpha_t, \beta_t) = \int_0^1 {\omega^w_t}^{\alpha_t - 1} \cdot (1 - \omega^w_t)^{\beta_t - 1} d\omega^w_t, \quad (30)$$

where, $0 \leq \omega^w_t \leq 1$ and $\alpha_t, \beta_t > 0$. Given a prediction of wind power $\bar{\omega}^w_t$ at time interval t, (28) models the possible uncertainty realizations ω^w_t. α_t and β_t are parameters of the Beta PDF and depend on the mean value $\bar{\omega}^w_t$ and the standard deviation σ_t according to the following expressions:

$$\alpha_t = \frac{(1 - \bar{\omega}^w_t) \cdot {\bar{\omega}^w_t}^2}{\sigma^2} - \bar{\omega}^w_t, \quad (31)$$

$$\beta_t = \frac{1 - \bar{\omega}^w_t}{\bar{\omega}^w_t} \cdot \alpha_t. \quad (32)$$

The relationship between $\bar{\omega}^w_t$ and σ_t is given by $\sigma_t = 0.5\bar{\omega}^w_t(1 - \bar{\omega}^w_t)$ [17]. The formulation of the Beta PDF for solar PV-based DG is the same as (29)-(32) with the variables changed accordingly.

B. Conventional load uncertainty

The forecast errors of the conventional load consumption are modeled using a normal PDF. Specifically, the possible realizations of the conventional load consumption $P^Z_{i,t,s}$, $P^I_{i,t,s}$ and $P^P_{i,t,s}$ are assumed to be normally distributed around the predicted value with a standard deviation of 2%.

C. Uncertainty of EVs

The arriving t^{arr}_m and departing t^{dep}_m times of each EV m are modeled using segmented normal distribution functions [18] as follows:

$$f_r(t^{dep}_m) = \begin{cases} \frac{1}{\sqrt{2\pi}\sigma_r} \exp\left[-\frac{\left(t^{dep}_m - \mu_r\right)^2}{2\sigma^2_r}\right], 0 < t^{dep}_m \leq (\mu_r + 12), \\ \frac{1}{\sqrt{2\pi}\sigma_r} \exp\left[-\frac{\left(t^{dep}_m - 24 - \mu_r\right)^2}{2\sigma^2_r}\right], (\mu_r + 12) < t^{dep}_m \leq 24, \end{cases} \quad (33)$$

$$f_e(t^{arr}_m) = \begin{cases} \frac{1}{\sqrt{2\pi}\sigma_e} \exp\left[-\frac{(t^{arr}_m + 24 - \mu_e)^2}{2\sigma^2_e}\right], 0 < t^{arr}_m \leq (\mu_e - 12), \\ \frac{1}{\sqrt{2\pi}\sigma_e} \exp\left[-\frac{(t^{arr}_m - \mu_e)^2}{2\sigma^2_e}\right], (\mu_e - 12) < t^{arr}_m \leq 24, \end{cases} \quad (34)$$

For each EV m, the travel mileage χ_m is described using a logarithmic normal distribution as follows:

$$f_d(\chi_m) = \frac{1}{\sqrt{2\pi}\sigma_d} \exp\left[-\frac{\left(\ln \chi_m - \mu_d\right)^2}{2\sigma^2_d}\right]. \quad (35)$$

The travel mileage χ_m is used to calculate the the SOC of the EV m at time t^{arr}_m. The shape of the PDFs (33)-(35) is defined by the following values: $\mu_r = 8.92$, $\sigma_r = 3.24$, $\mu_e = 17.47$, $\sigma_e = 3.41$, $\mu_d = 2.98$, $\sigma_d = 1.14$ [18].

D. Scenarios generation

A scenario generation and reduction process is used to obtain a set of scenarios that efficiently approximates the PDFs that model the system's uncertainties. Initially, a large set of scenarios, each with the same probability of occurrence, is sampled from the PDFs. Then, the simultaneous backward reduction technique [19] is applied to obtain a reduced set of scenarios each with probability of occurrence ρ_s. In this way, it is possible to accurately take into account uncertainties ensuring that the optimization problem can be solved using viable computational resources.

IV. Case study and simulations results

This section describes the setup for the case study and discusses the simulations results. The model was implemented in the algebraic modeling language AMPL and solved using the solver CPLEX.

A. Technical data and specifications

Simulation results were obtained from a 33-bus test system whose topology and data can be found in [15]. This EDS has peak active load consumption of 3.715 MW and nominal voltage of 12.66 kV. The substation transformer has a capacity of 5 MVA and is installed with an OLTC that is capable of regulating $\pm 5\%$ of input voltage in steps of $\Delta tap_i =$

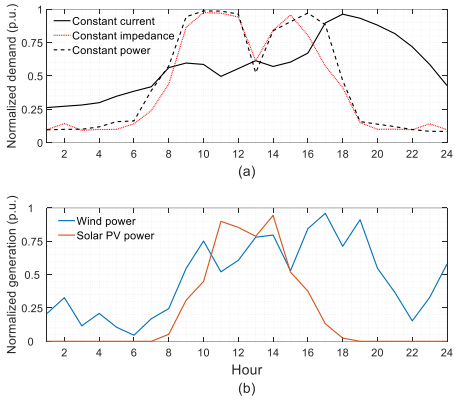

Fig. 1: Predicted profiles of a) conventional load consumption and b) Renewable-based DG production.

$0.0125\ p.u.$ with $\overline{tap} = 4$. The number of switching operations of the OLTC during the day is limited to 16 (i.e., $N_i^{tp} = 16$). The bus voltages are limited to maximum and minimum values of 1.05 and 0.95 p.u., respectively. The participation of the constant impedance, constant current and constant power load components in the total conventional load is considered to be 40%, 40% and 20%, respectively. Wind-based DG is installed at buses 14 and 20, both with rated capacity of 1.25 MW. Solar PV-based DG with rated capacity of 1.5 MW is installed at bus 28. The EDS supplies a population of 212 EVs aggregated in the same proportion at buses 18, 22, 25 and 33. The type of EV considered is Nissan Leaf with battery capacity of 40 kWh, charging power of 7 kW, discharging power of 3.5 kW, average consumption of 0.3 kWh/mi, and charging discharging efficiencies of 100% [20].

Predictions of conventional load consumption, solar PV-based DG power production, and wind-based DG power production are shown in Fig. 1. Using these predictions, 1000 scenarios are randomly generated using the PDFs presented in section III. Then, the simultaneous backward reduction technique was applied to reduce the scenario number to 10. To asses the impact of the optimal dispatch of aggregated EVs to reduce the consumption of voltage dependent loads and the energy losses the following cases are defined:

1) Case I: OLTC operation without optimal EVs dispatch. This case considers that the EVs are charged at maximum rate once they are plugged into the EDS.
2) Case II: OLTC operation and optimized power absorption of aggregated EVs. This case assumes that the EVs can only be charged.
3) Case III: OLTC operation and optimized power absorption and injection of aggregated EVs. This case considers EVs with V2G technology that can be charged and discharged.

B. Results

Since the optimization problem is evaluated over a set of scenarios, the presented power, energy and voltage results correspond to expected values over all simulated scenarios. The energy savings that can be achieved during the day through the optimal dispatch of aggregated EVs are shown in

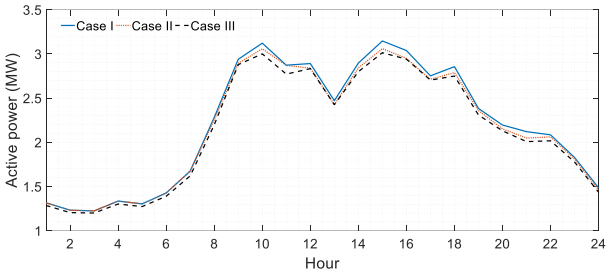

Fig. 2: Daily profiles of conventional load consumption plus energy losses.

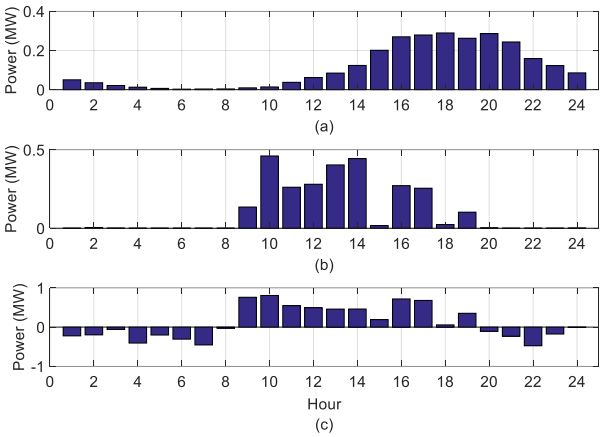

Fig. 3: Power exchanges of the EVs population for cases a) I, b) II and c) III.

Fig. 2. The total expected energy consumption (conventional load consumption plus losses) for cases I, II and III is 52.88 MWh, 52.10 MWh and 51.27 MWh, respectively. It is observed that, by optimizing the power absorbed by the aggregated EVs in case II, it is possible to reduce the energy consumption by 1.48% compared to case I. When the EVs can also inject power into the EDS in case II, the energy savings increase to 3.04%.

The power exchanged by the EVs population at each hour for the three cases is shown in Fig. 3. In Fig. 4 are shown the OLTC tap positions at each hour for the three cases. In case I, without optimal dispatch the EV population consumption concentrates between hours 12-24. This behavior is determined by the EV arriving times and the initial SOC of their batteries. In case II, the power supplied to the EVs is shifted to the hours with high generation. In this case, the optimized dispatch of the EVs complements the operation of the OLTC. From Fig. 4, it is observed that lower tap positions are obtained in case II compared to case I. This reason for this is that the power absorbed by the EVs aggregated at each node is controlled to flatten the net demand profile (generation minus demand) in the EDS along the day, which helps to lower the OLTC tap position requiring the same number of switching operations. In case III, the EVs inject power into the EDS at hours with low generation and absorb power at hours of high generation. This results in a flatter net demand profile than in case II, which allows the OLTC tap to be switched to lower positions

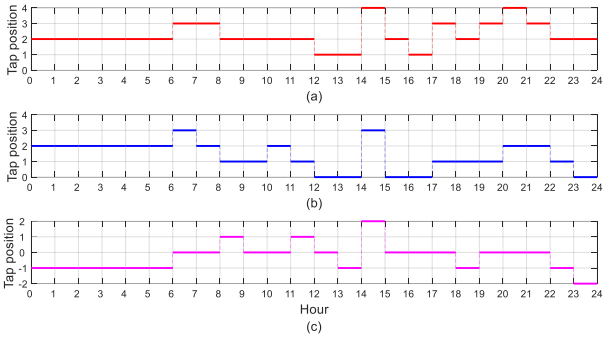

Fig. 4: OLTC tap positions for cases a) I, b) II and c) III.

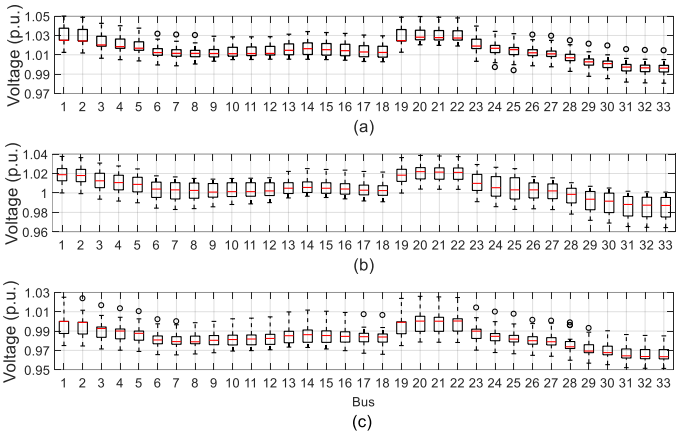

Fig. 5: Voltage profiles for cases a) I, b) II and c) III.

as observed in Fig. 4.

FiG. 5 shows the voltage profiles for the three cases. Each boxplot summarizes for each bus the voltage magnitudes for the 24-hours period. In case I, the voltage levels remain above the nominal most of the time for most buses, reaching a minimum value of about 0.98 p.u. at bus 33. In case II, the voltage levels are lowered reaching a minimum value of about 0.965 p.u. at bus 33. In case III, it is possible to lower the voltage levels to values below the nominal most of the time for most buses. In this case the minimum voltage is close to 0.95 p.u. but still remains withing the specified limits.

C. Conclusions

A Volt-Var optimization model that includes the coordinated dispatch of aggregated EVs for CVR implementation in MV EDSs was proposed. EVs were model as clustered at specific EDS nodes taking into account technical characteristics and the driving pattern of individual EVs. Uncertainties related to prediction errors of solar PV and wind-based DG power production, conventional load consumption and EV driving patterns were taken into account through a two-stage stochastic programming formulations. Results showed that by including the coordinated dispatch of EVs is possible to obtain deeper voltage reductions than with the OLTC operating alone, which translates in higher energy savings. About 3% of energy savings were obtained coordinating the power absorbed and injected by the EVs. For future works it is pretended to investigate the reactive power support by EVs for voltage regulation in the EDS.

REFERENCES

[1] A. Padilha-Feltrin, D. A. Quijano Rodezno, and J. R. S. Mantovani, "Volt-var multiobjective optimization to peak-load relief and energy efficiency in distribution networks," *IEEE Trans. Power Del.*, vol. 30, no. 2, pp. 618–626, 2015.

[2] Z. Wang and J. Wang, "Time-varying stochastic assessment of conservation voltage reduction based on load modeling," *IEEE Trans. Power Syst.*, vol. 29, no. 5, pp. 2321–2328, 2014.

[3] ——, "Review on implementation and assessment of conservation voltage reduction," *IEEE Trans. Power Syst.*, vol. 29, no. 3, pp. 1306–1315, 2014.

[4] D. A. Quijano and A. Padilha-Feltrin, "Optimal integration of distributed generation and conservation voltage reduction in active distribution networks," *Int. J. Electr. Power Energy Syst.*, vol. 113, pp. 197–207, 2019.

[5] R. W. Uluski, "Vvc in the smart grid era," in *IEEE PES General Meeting*, 2010, pp. 1–7.

[6] Q. Zhang, K. Dehghanpour, and Z. Wang, "Distributed cvr in unbalanced distribution systems with pv penetration," *IEEE Trans. Smart Grid*, vol. 10, no. 5, pp. 5308–5319, 2019.

[7] S. Singh, V. Babu Pamshetti, A. K. Thakur, and S. P. Singh, "Multistage multiobjective volt/var control for smart grid-enabled cvr with solar pv penetration," *IEEE Syst. J.*, vol. 15, no. 2, pp. 2767–2778, 2021.

[8] Y. Zhang, Y. Xu, H. Yang, and Z. Y. Dong, "Voltage regulation-oriented co-planning of distributed generation and battery storage in active distribution networks," *Int. J. Electr. Power Energy Syst.*, vol. 105, pp. 79–88, 2019.

[9] D. Choeum and D.-H. Choi, "Vulnerability assessment of conservation voltage reduction to load redistribution attack in unbalanced active distribution networks," *IEEE Trans. Ind. Informat.*, vol. 17, no. 1, pp. 473–483, 2021.

[10] M. S. Hossan and B. Chowdhury, "Integrated cvr and demand response framework for advanced distribution management systems," *IEEE Trans. Sustain. Energy*, vol. 11, no. 1, pp. 534–544, 2020.

[11] D. A. Quijano, O. D. Melgar-Dominguez, C. Sabillon, B. Venkatesh, and A. Padilha-Feltrin, "Increasing distributed generation hosting capacity in distribution systems via optimal coordination of electric vehicle aggregators," *IET Gener., Trans. Dist.*, vol. 15, no. 2, pp. 359–370, 2021.

[12] S. Li, C. Gu, J. Li, H. Wang, and Q. Yang, "Boosting grid efficiency and resiliency by releasing v2g potentiality through a novel rolling prediction-decision framework and deep-lstm algorithm," *IEEE Syst. J.*, vol. 15, no. 2, pp. 2562–2570, 2021.

[13] S. Singh, V. B. Pamshetti, and S. P. Singh, "Time horizon-based model predictive volt/var optimization for smart grid enabled cvr in the presence of electric vehicle charging loads," *IEEE Trans. Ind. Appl.*, vol. 55, no. 6, pp. 5502–5513, 2019.

[14] H. Gharavi, G. McLorn, X. Liu, and S. McLoone, "Coordinating ev charging and dynamic cvr in a lv network: A uk case study," *IFAC-PapersOnLine*, vol. 51, no. 10, pp. 193–198, 2018.

[15] M. Baran and F. Wu, "Network reconfiguration in distribution systems for loss reduction and load balancing," *IEEE Trans. Power Del.*, vol. 4, no. 2, pp. 1401–1407, 1989.

[16] L. Gan, N. Li, U. Topcu, and S. H. Low, "Exact convex relaxation of optimal power flow in radial networks," *IEEE Trans. Autom. Control*, vol. 60, no. 1, pp. 72–87, 2015.

[17] H. Bludszuweit, J. A. Dominguez-Navarro, and A. Llombart, "Statistical analysis of wind power forecast error," *IEEE Transactions on Power Systems*, vol. 23, no. 3, pp. 983–991, 2008.

[18] W. Yao, J. Zhao, F. Wen, Y. Xue, and G. Ledwich, "A hierarchical decomposition approach for coordinated dispatch of plug-in electric vehicles," *IEEE Transactions on Power Systems*, vol. 28, no. 3, pp. 2768–2778, 2013.

[19] H. Heitsch and W. Römisch, "Scenario reduction algorithms in stochastic programming," *Comput. Optim. Appl.*, vol. 24, no. 2, 2003.

[20] PodPoint, "Electric vehicle guide." Accessed February. 27, 2022. [Online]. Available: https://pod-point.com/guides/vehicles?